Upper atmosphere radiance data assimilation: Observing system simulation experiments for GOLD far ultraviolet observations

Clayton Cantrall[1], Tomoko Matsuo[1], and Stan Solomon[2]

[1]University of Colorado, Boulder
[2]National Center for Atmospheric Research

November 23, 2022

Abstract

Availability of far ultraviolet observations of Earth's dayglow by the NASA Global-scale Observations of the Limb and Disk (GOLD) mission presents an unparalleled opportunity for upper atmosphere data assimilation. Assimilation of the observed dayglow emissions can be formulated in a similar fashion to lower atmosphere radiance data assimilation approaches using the sensitivity of the Lyman-Birge-Hopfield (LBH) band emission to thermospheric temperature. To demonstrate such an approach, we present a proof-of-concept implementation of an ensemble square-root filter measurement update step using ensemble simulation of the thermosphere and LBH emission by the NOAA's Whole Atmosphere Model (WAM) and NCAR's Global Airglow model. With help of a new assimilation approach, the utility of GOLD observations can be extended to reveal the global, time-dependent, altitude-resolved thermospheric structure, offering the key to addressing a number of outstanding questions such as origins of traveling atmospheric disturbances.

Upper atmosphere radiance data assimilation: Observing system simulation experiments for GOLD far ultraviolet observations

AGU 100 FALL MEETING Washington, D.C. | 10–14 Dec 2018

Clayton Cantrall[1], Tomoko Matsuo[1], Stan Solomon[2]

[1]Department of Aerospace Engineering Sciences, University of Colorado – Boulder, USA, [2]High Altitude Observatory, National Center for Atmospheric Research, Boulder, Colorado, USA

Contact: clayton.cantrall@colorado.edu

Formulation of GOLD Radiance Data Assimilation

Background

Availability of far ultraviolet observations of Earth's dayglow by the NASA Global-scale Observations of the Limb and Disk (GOLD) mission presents an unparalleled opportunity for upper atmosphere data assimilation. **Assimilation of the observed dayglow emissions can be formulated in a similar fashion to lower atmosphere radiance data assimilation approaches using the sensitivity of the Lyman-Birge-Hopfield (LBH) band emission to thermospheric temperature.** To demonstrate such an approach, we present a proof-of-concept implementation of an ensemble square-root filter measurement update step using ensemble simulation of the thermosphere and LBH emission by the NOAA's Whole Atmosphere Model (WAM) and NCAR's Global Airglow model. With help of a new assimilation approach, the utility of GOLD observations can be extended to reveal the global, time-dependent, altitude-resolved thermospheric structure, offering the key to addressing a number of outstanding questions such as origins of travelling atmospheric disturbances.

Problem Statement

The measurement update objective is to estimate the hidden state of temperature at h discrete altitude levels, here denoted as x, from a vector of k observations denoted by y. An ensemble data assimilation approach allows us to account for the realistic non-local and non-linear relationship of LBH emissions to temperature when assimilating the GOLD measurements. The ensemble square root filters uses sample statistics from an ensemble of model forecasts to determine the impact that observations have on the inference of model state variables.

GOLD Sensitivity to Temperature

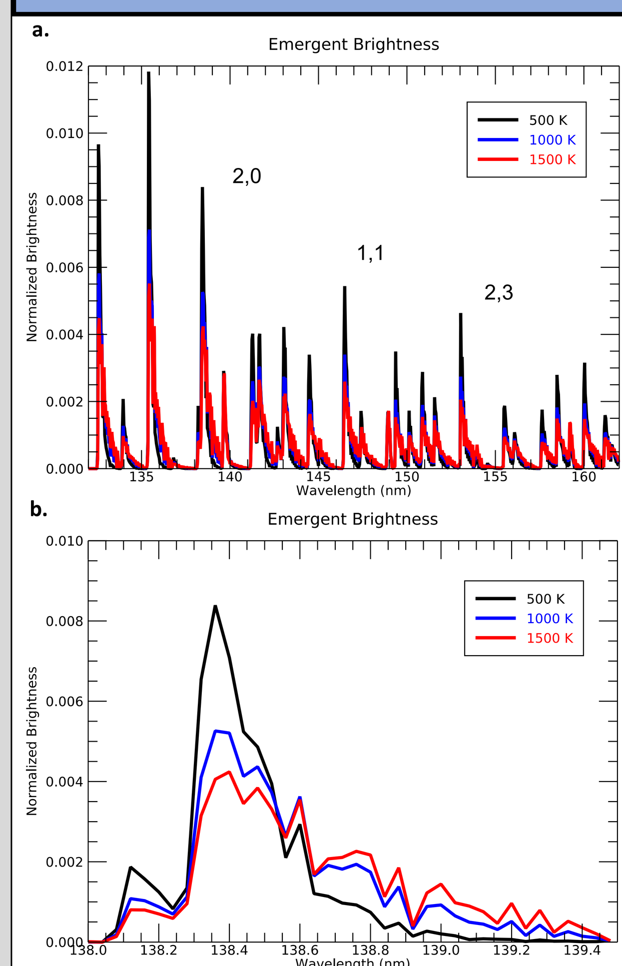

Figure 1 - (a) Simulated N_2 Lyman-Birge-Hopfield emissions between the GOLD bandwidth of 132 and 162 nm at three reference temperatures. The specified (2,0), (1,1), and (2,3) vibrational transitions are those assimilated. (b) Simulated N_2 Lyman-Birge-Hopfield emissions between 138 and 139.5 nm centered around (2,0). **The temperature dependence is observed by the broadening of the (2,0) feature with increased temperature (Aksnes et al., 2006; Eastes et al., 2011).**

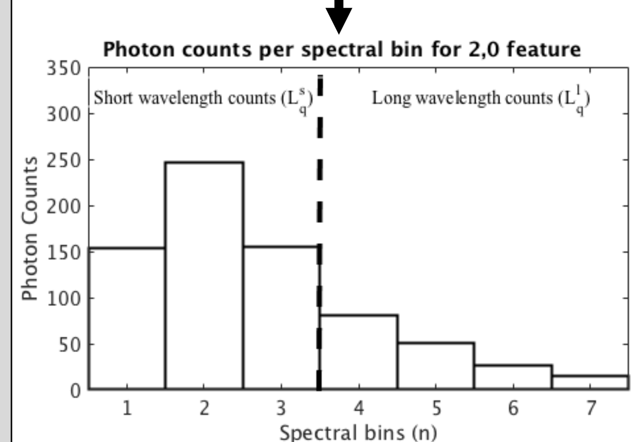

Figure 2 – Synthetic GOLD observation of 2,0 emission feature. L_q^s is the sum of the photon counts for the so-called "short" wavelength bins. L_q^l is the sum of the counts of the remaining "long" wavelength bins.

The assimilated observation, y, is L_q^s/L_q^l.

Assimilation with Ensemble Square Root Filter (EnSRF)

Important components of the ensemble transform implementation are two sets of ensemble: the prior (forecast model) ensemble $\{x_f^1 \dots x_f{}^m\}$ and prior observation ensemble $\{y_f^1 \dots y_f{}^m\}$ where y_f denotes predicted GOLD observations from the model state x_f. The covariance of x is approximated by the m-member ensemble $x^1, \dots, x^m$ as follows (Anderson et al. (2003)).

$$P \approx D_x D_x^T \quad \longrightarrow \quad D_x = \frac{1}{\sqrt{m-1}}[(x'^1) \dots (x'^m)]$$

Note that the rank of P is at most $m-1$ and $h > m$. D_x is composed of the mean-subtracted temperature of the ensemble i^{th} ensemble member$(x'^i = x^i - \bar{x})$. In the update step, the prior (forecast) ensemble is transformed to the posterior (analysis) ensemble. **The implementation is as follows:**

General EnSRF Measurement Update

1. Create the $h \times m$ data matrices D_x and D_y as:

$$D_x = \frac{1}{\sqrt{m-1}}[(x_f'^1) \dots (x_f'^m)]$$

$$D_y = \frac{1}{\sqrt{m-1}}[(y_f'^1) \dots (y_f'^m)]$$

2. Update the ensemble mean using observation y_j, with its error variance R_{jj} in observation space:

$$\overline{y_{a_j}} = \overline{y_{f_j}} + \frac{D_{y_j} D_{y_j}{}^T}{D_{y_j} D_{y_j}{}^T + R_{jjkk}} (y_j - \overline{y_{f_j}})$$

3. Update each ensemble member ($i = 1, \dots, m$)

$$y_{a_j}^i = \sqrt{\frac{R_{jjkk}}{R_{jjkk} + D_{y_{jk}} D_{y_{jk}}{}^T}} \left(y_{f_{jk}}^i - \overline{y_{f_j}}\right) + \overline{y_{a_j}}$$

4. Update each ensemble member in state space

$$x_{a_j}^i = x_{f_j}^i + \frac{D_x D_{y_j}{}^T}{D_{y_j} D_{y_j}{}^T} (y_{a_j}^i - y_{f_j}^i)$$

5. Repeat steps 1-4 for each observation $y_1, y_2, \dots y_k$. At the end of j^{th} iteration the intermediate analysis ensemble becomes the forecast ensemble ($\{x_{a_j}^1 \dots x_{a_j}^i\} \rightarrow \{x_f^1 \dots x_f{}^m\}$) for the $j+1$ iteration. After the k iterations, $\{x_{a_k}^1 \dots x_{a_k}^i\} = \{x_a^1 \dots x_a^m\}$ for that time of observation. The ensemble mean serves as the data assimilation analysis.

GOLD Temperature Measurement Update

1. $\{x_f^1 \dots x_f{}^m\}$: Temperature defined by NOAA WAM (Akmaev, 2011) ensemble.

$\{x_f^1 \dots x_f{}^m\}$ ➡ Light grey in Figure 3

$\{y_f^1 \dots y_f{}^m\}$: $\{x_f^1 \dots x_f{}^m\}$ through forward model.

2. y_j**:** Compute ratio of (2,0), (1,1), (2,3) emission features from Level 1C data.

3-4. Update temperature profile for each WAM ensemble member.

$\{x_a^1 \dots x_a{}^m\}$ ➡ Dark grey in Figure 3

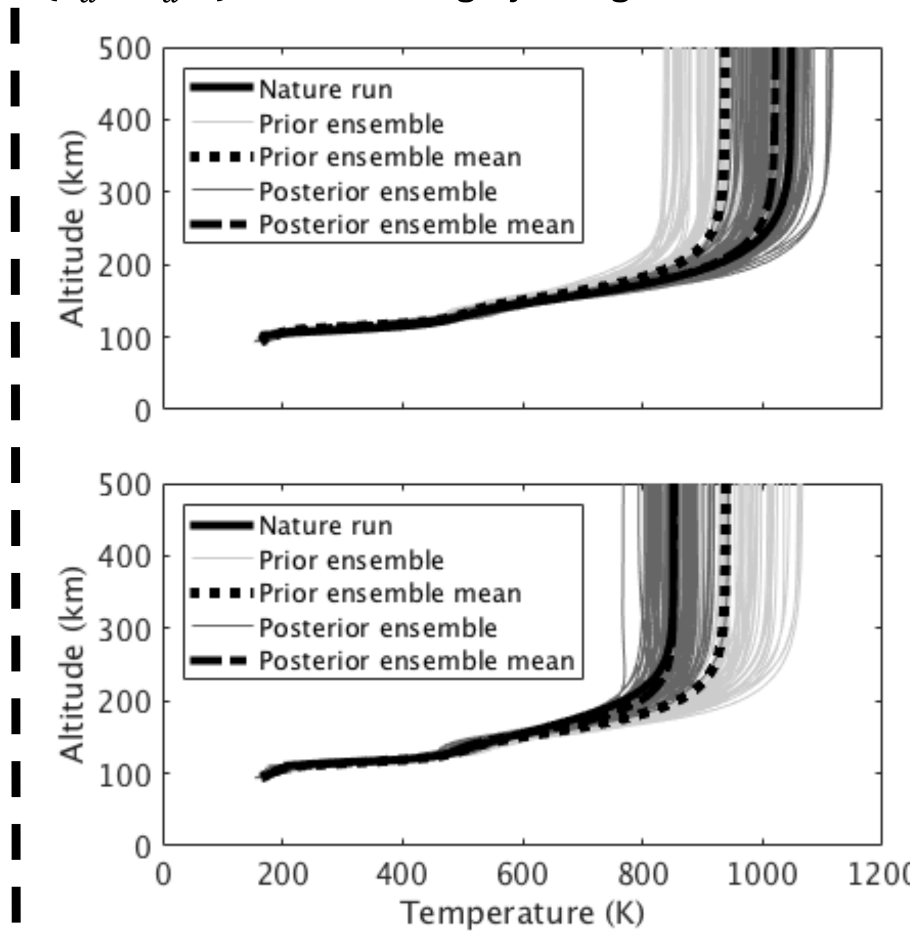

Figure 3 – **Example of posterior temperature profile estimates** in the nadir direction when the truth temperature is above and below the forecast model temperature. The solid black line represents the TIEGCM nature run that produced synthetic observations. Instrument noise effects are included in generating the truth observations.

Forward Model: State Space to Observation Space

The data assimilation requires an observation operator that maps the model state, x, to GOLD measurements, y: $\quad y = H(x) + \epsilon$

Model state, x → NCAR Global Airglow (GLOW) model (Solomon, 2017) → NCAR GOLD line-of-sight (LOS) model → Instrument Model → Observation, y

Observation System Simulation Experiments (OSSEs)

OSSE Set Up

Synthetic measurements were generated by passing "nature" runs of the Thermosphere Ionosphere Electrodynamic General Circulation Model (TIEGCM) (Qian et al., 2014) through the forward model with the addition of Poisson and background noise. The accuracy of the posterior temperature estimate is tested by comparison to the nature run.

Case Study: Quiet Time Performance

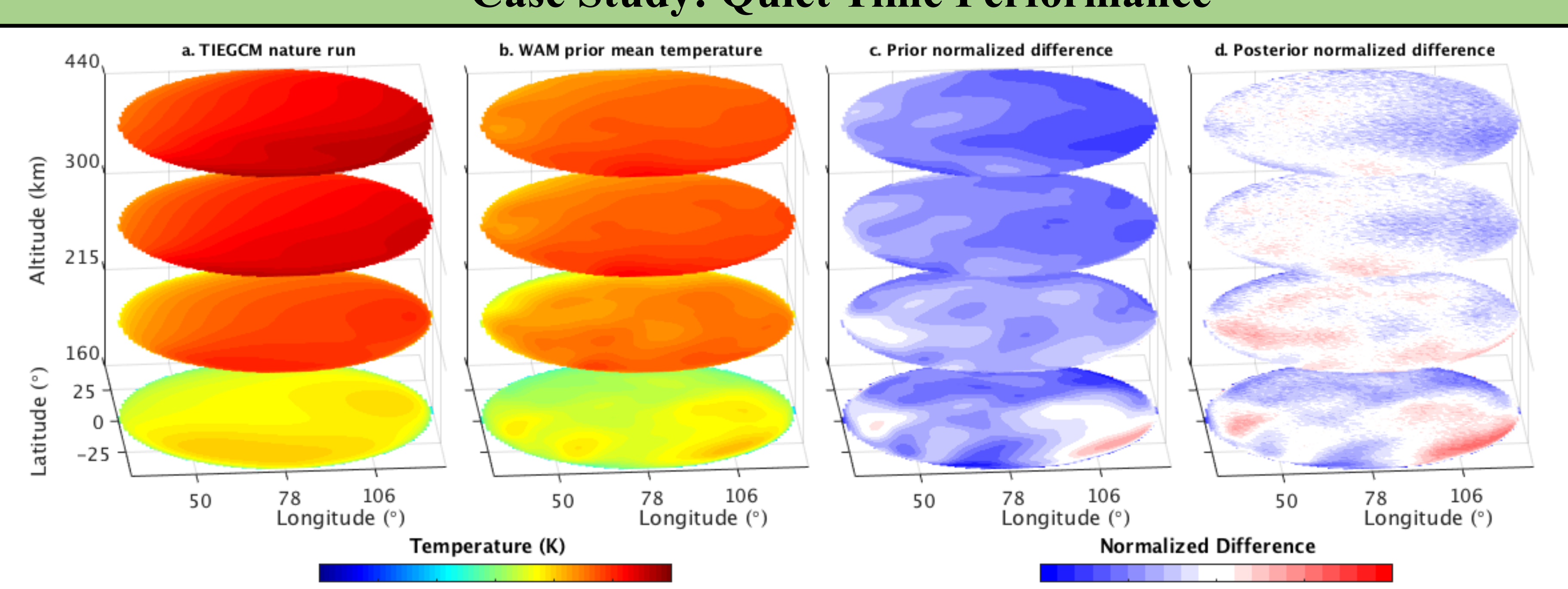

Figure 4 – 3-Dimensional plots showing (a) the TIEGCM nature run temperature, (b) the forecast estimate, (c) the normalized difference between the nature run and forecast estimate, and (d) the normalized difference between the nature run and analysis estimate. **The mean normalized difference of the analysis estimate over the disk is <2.5% above 200 km altitude and increases to a max of 15% near 160 km.**

Case Study: Storm Time Performance

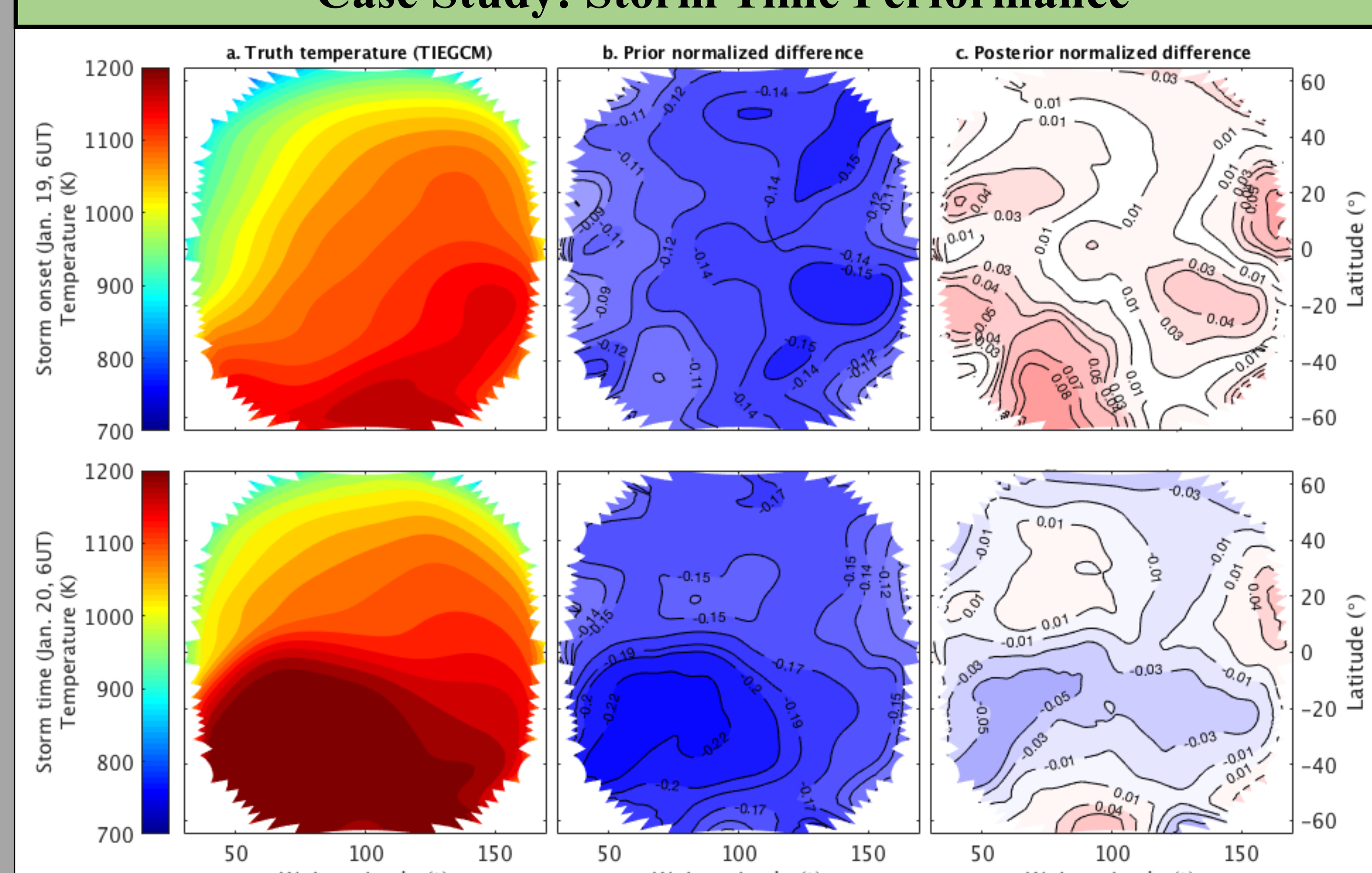

Figure 5 – (a) The truth temperature at 300 km altitude at the onset and of the geomagnetic storm (top) and during the peak response (bottom). (b) There is a high normalized difference (> 20%) during the peak response of the thermosphere. (c) **The difference is significantly reduced over the disk (< 5%) after the observation is assimilated.**

Results and Conclusions

- Proof-of-concept implementation of an ensemble filter to assimilate satellite far ultraviolet observations of Earth's dayglow.
- **Observation system simulation experiments suggest temperature assimilation analysis in accuracy of 35 K (nadir) and ~60 K (average) over Earth's disk.**
- **Thermospheric temperature biases in models can be reduced by 97% under geomagnetically quiet conditions and by 87% under disturbed conditions.**
- The data assimilation methods' reliance on the prior information, means the posterior temperature profile along a line-of-sight will not significantly deviate from the temperature structure specified by the forecast ensemble.
- The radiance data assimilation approach demonstrated in this paper presents opportunities to reconstruct large-scale and medium-scale transient features like TADs generated by magnetospheric forcing and upward propagating gravity waves.
- **The study is a first step to assimilate the GOLD disk image observations in a similar manner to lower atmosphere radiance data assimilation approaches.**

References

[1] Akmaev, R. A. Rev. Geophys., 49, 2011. [2] Solomon, S. Journal of Geophysical Research - Space Physics, 122, 2017. [3] Aksnes, A. et al. Geophysical Research Letters, 33, 2006. [4] Eastes, R. J. Geophys. Res., 116, 2011. [5] Anderson, J.L. Mon. Weather Rev., 129, 2884-2903, 2003. [6] Qian, L. Geophys. Monogr. Ser., vol. 201, 2014.

Acknowledgements: This study is supported by the NASA award NNX14AI17G. We would like to thank Richard Eastes for sharing his extensive knowledge of the GOLD mission and GOLD's temperature sensitivity which made this work possible.